ACS Medicinal Chemistry Letters

Letter

pubs.acs.org/acsmedchemlett

New Hits as Antagonists of GPR103 Identified by HTS

Anneli Nordqvist,[†] Lisbeth Kristensson,[‡] Kjell E. Johansson,[†] Krystle Isaksson da Silva,[†] Tomas Fex,[†] Christian Tyrchan,[§] Anette Svensson Henriksson,[†] and Kristina Nilsson*[,†]

[†]CVMD Medicinal Chemistry, [‡]Discovery Sciences, and [§]RIA Medicinal Chemistry, AstraZeneca, Pepparedsleden 1, 431 83 Mölndal, Sweden

Supporting Information

ABSTRACT: Preclinical data indicate that GPR103 receptor and its endogenous neuropeptides QRFP26 and QRFP43 are involved in appetite regulation. A high throughput screening (HTS) for small molecule GPR103 antagonists was performed with the clinical goal to target weight management by modulation of appetite. A high hit rate from the HTS and initial low confirmation with respect to functional versus affinity data challenged us to revise the established screening cascade. To secure high quality data while increasing throughput, the binding assay was optimized on quality to run at single concentration. This strategy enabled evaluation of a larger fraction of chemical clusters and singletons delivering 17 new compound classes for GPR103 antagonism. Representative compounds from three clusters are presented. One of the identified clusters was further investigated, and an initial structure−activity relationship study is reported. The most potent compound identified had a pIC_{50} of 7.9 with an improved ligand lipophilic efficiency.

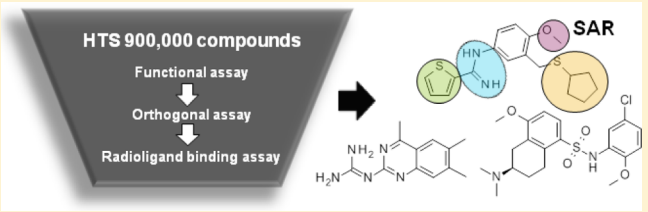

KEYWORDS: *G-protein coupled receptor, high throughput screening, appetite regulation, SP9155, 26RFa, 43RFa, GPCR*

Obesity is a global epidemic associated with increased morbidity and mortality.[1,2] GPR103 is a family A G-protein coupled receptor first described in 2001.[3] The endogenous GPR103 neuropeptide ligands QRFP26 and the *N*-terminal elongated QRFP43 were discovered by three different groups[4−6] and paired with an, at that time, orphan receptor GPR103.[4,5] QRFP26 and QRFP43 are RFamide peptides encompassing the C-terminal Arg-Phe-NH_2 motif common to all RFamide family members. Structure−activity relationships (SAR) studies of QRFP26 show that the terminal Phe_{24}-Arg_{25}-Phe_{26} motif[7] and the C-terminal amidation common to the RFamide family are very important for functional activity.[5,7]

Gene expression data show that GPR103 and its endogenous GPR103 neuropeptide ligands are expressed in ventromedial nuclei, lateral hypothalamus, and arcuate nucleus, which are areas known to be involved in the control of feeding behavior and body weight.[4,5,8−10] Peripherally GPR103 is found to be expressed in heart, kidney, retina, and testis but at considerably lower levels.[4] Preclinical data demonstrate that intracerebroventricular injections (i.c.v.) of the endogenous agonists QRFP26 and QRFP43,[6,10,11] as well as synthetic peptidomimetic agonists[12] increase feeding in rodents. Also, prepro-QRFP26 mRNA is up-regulated in the hypothalamus in fasted mice as well as in ob/ob and in db/db mice compared to fed mice and wild-type mice.[10] High-fat feeding of rats also results in increased expression of endogenous ligands but does not alter GPR103 expression. Data taken together points at GPR103 to have a function in controlling appetite, suggesting that inhibition of the orexigenic effect from QRFP26/QRFP43 receptor activation would promote reduced body weight by modulation of appetite.

Antagonists of GPR103 in context of weight management have previously been published in four different patents covering indole[13−15] and imidazoline[16] derivatives. In this communication we describe an HTS based hit identification of three novel GPR103 small molecule antagonists structurally distinct from previously disclosed GPR103 antagonists. A SAR study with synthetic procedures outlined for one of the most compelling clusters is presented.

The hit finding strategy for GPR103 antagonists was based on the HTS of the AstraZeneca proprietary compound collection. The primary assay in the screening cascade was a functional assay assessing GPR103 antagonism through measurements on production of inositol-1-phosphate (IP-1). Screening of compounds started at single concentration giving a hit rate of 4.7%. Functional activity was then followed up in a ten point concentration−response (CR) IP-1 assay leaving 83% classified as actives. Subsequently compounds were screened in an orthogonal cell based label free dynamic mass redistribution (DMR) ten point CR assay, in which 52% were confirmed active. Finally 100 compounds based on a diverse selection of the most attractive compounds were tested in a [^{125}I]-QRFP43 radioligand binding (RLB) ten point CR assay with a hit rate of 3%. Despite a high confirmation rate of functional activity, only a small fraction of compounds considered active in the

Received: December 17, 2013
Accepted: February 22, 2014
Published: February 22, 2014

functional assays were confirmed in the RLB assay. This low confirmation rate could have several reasons, e.g., due to the lack of a technology artifact assay in IP-1, binding to allosteric sites of GPR103, or IP-1 production through interaction with other protein targets. To ensure high quality starting points for the chemistry program, we therefore needed to assess a larger part of the chemical space of the HTS output by affinity screening in the [^{125}I]-QRFP43 RLB assay.

The throughput of the original [^{125}I]-QRFP43 96-well format RLB assay ten point CR setup was hampered by high cost per well, amount of radioactive waste, and by variability in quality control parameters. Hence, when affinity data became critical for project progression the RLB assay quality had to be improved to allow counter screening of a larger set of compounds in single concentration screening and thereby increase the throughput. This was achieved by the transfer of larger volumes of the assay reaction to the filter plate. This step was performed by an automated filtration step in a Biomek FX (Beckman Coulter) where the assay reaction is transferred to a filter plate and all wells in the plate are washed simultaneously with ice-cold wash buffer under vacuum to remove all unbound radioligand. By further optimizing the number of wash cycles and the height of the Biomek FX tip head over the filter plate during washing, the background radioactivity was decreased, thus increasing the assay window. This was reflected by the Z' values increasing from 0.2−0.3 to 0.5−0.9 (average 0.76 ± 0.11, mean 0.76, n = 24). The quality of the improved assay was controlled with 29 GPR103 reference compounds previously confirmed in functional and affinity screening.

By revisiting all compounds flagged as active in IP-1 single concentration in the HTS and in ten point CR, 963 compounds were selected for screening in the [^{125}I]-QRFP43 RLB assay single concentration to give a mean inhibition of radioligand binding in percent at 10 μM ligand concentration. The compounds considered active, 12.8%, were subsequently followed up in RLB ten point CR. The accuracy of the single concentration RLB assay was 83% calculated as (TP + TN)/(TP + TN + FP + FN), as confirmed in ten point CR RLB. This approach enlarged the set of confirmed GPR103 antagonists and enabled us to identify in all 17 new chemical clusters of which representatives from three of the clusters are depicted in Table 1. From a SAR perspective, these structures are novel with respect to chemical similarity compared with previously known GPR103 antagonists. A common feature of the presented clusters in Table 1 is their basic functionality with pK_a ranging from 8.1−10.5, also observed in the endogenous agonists[5−7] as well as in pseudopeptide agonists.[12,19] Two of the identified cluster representatives (**2** and **3**, Table 1) have previously been reported in the context of ligands for GPCRs.[17,18] Compound **1** showed compelling in vitro data on GPR103 antagonism as well as potential for exploration and was selected as a starting point for chemistry. Full IC_{50} curves for IP-1 and RLB assays of compound **1** are depicted in Figures S1 and S2 in the Supporting Information.

To build SAR around the core structure of compound **1** (Table 2, see Supporting Information for Table 2 with structures drawn) the following parts were modified: (I) the amidine aryl group, (II) the amidine functionality, (III) the methoxy substituent, and (IV) the cyclopentylsulfanylmethyl group (Schemes 1−5).

Exploration of the amidine aryl group (I) in the hit compound **1** (Scheme 1), was started with bromomethylation of the commercially available 4-methoxy-nitrobenzene (**4**)

Table 1. Cluster Representatives from the HTS

	IP-1		RLB		
		No.[b]			
Compound	pIC_{50}[a]	pIC_{50}>5	pIC_{50}[a]	log$D_{7.4}$	pK_a
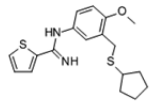 1	7.3± 0.2 (4)	13	6.8± 0.2 (3)	3.3± 0.1 (3)	8.1
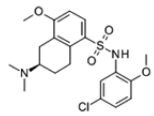 2[17]	7.1± 0.1 (3)	29	7.1± 0.1 (3)	2.3± 0.1 (3)	10.5
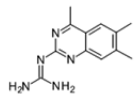 3[18]	5.6± 0.02 (3)	8	5.3± 0.3 (3)	<0.6 (2)	9.3

[a]pIC_{50} is reported as mean ± SD, n = 2 − 4 from ten point CR with the number of experiments in parentheses. [b]Number of cluster members with pIC_{50} > 5 in IP-1 after HTS.

followed by reaction with cyclopentanethiol and reduction of the nitro group to give **6**. The resulting aniline was reacted with selected nitriles to give the desired amidines (**1**, **7a**−**7k**).

Amidine aryl and alkyl analogues to compound **1** (**7a**−**7k**, Scheme 1, Table 2) display a broad SAR. The thiophene-3-yl regioisomer (**7a**), the phenyl-analogue (**7b**), 4- or 5-substituted thiophene (**7c**−**7e**), or the *para*-chlorophenyl analogue (**7f**) are equipotent or more potent compared to the thiophen-2-yl hit (**1**) with pIC_{50} in the range of 6.8−7.9. Replacing the thiophene with the more polar, electron poor thiazole (**7i**) or *para*-pyridine (**7j**) gave marked reduction in potency. However, introducing a *meta*-pyridine (**7k**) gains back some of the potency compared to **7i** and **7j**, while keeping log$D_{7.4}$ at 2.6. A striking drop in or loss of IP-1 activity was seen in benzyl- and ethyl-matched pairs to compound **1**, **7g** (pIC_{50} 5.2) and **7h** (pIC_{50} <4.4) respectively, suggesting that the amidine aryl group should be directly adjacent to the amidine.

Variations of the amidine functional group (II) in compound **1** were introduced by coupling **6** with thiophene-2-carboxylic acid to give the amide analogue (**8**) or with 2-fluoropyridine to give the 2-aminopyridine analogue (**10**, Scheme 1). The amidine functionality was further modulated by mono-*N*- and di-*N*,*N*-methylation starting from the thiophene carboxamide **8**. Compound **8** was transformed to the corresponding carbothioamide using Lawesson reagent and then *N*-alkylated by reaction with methyl amine to give mono-*N*-methylated **9a** and di-*N*,*N*-methylated compound **9b** (Scheme 1).

From SAR exploration modulating the amidine, it is evident that a positive charge on the amidine is a hot-spot for targeting GPR103 antagonism also consistent with the pK_a properties of the hit compounds (**2** and **3**). By replacing the amidine with the corresponding amide (**8**) or the 2-aminopyridyl analogue (**10**), the compounds drop 2 orders of magnitude in potency compared to the original amidine hit (**1**). Also, methylation of the imine nitrogen of the amidine (**9a**) leads to one log unit drop in functional activity, whereas methylation of both the amidine nitrogens (**9b**) abolishes functional activity (Table 2).

dx.doi.org/10.1021/ml400519h | ACS Med. Chem. Lett. 2014, 5, 527−532

Table 2. Functional Activity and Radioligand Binding for Analogues of Compound 1 and Their Measured $logD_{7.4}$

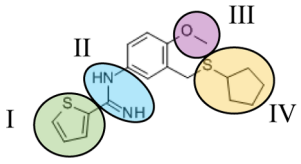

Cmpd	IP-1[a] pIC_{50}	RLB[a] pIC_{50}	$logD_{7.4}$	LLE[b]
I				
1	7.3±0.2 (4)	6.8±0.2 (3)	3.3±0.1 (3)	4.0
7a	7.0±0.04 (3)	6.9±0.04 (2)	2.5±0.1 (2)	4.5
7b	7.7±0.2 (3)	7.6±0.1 (2)	2.5±0.3 (4)	5.2
7c	7.2±0.02 (3)	7.0±0 (2)	3.7±0.1 (2)	3.5
7d	6.8±0.1 (3)		4.7±0.6 (2)	2.1
7e	7.7±0.2 (2)	6.9±0.2 (3)	>5 (2)	<2.7
7f	7.9 (1)	7.4±0.2 (3)	3.7±0 (2)	4.2
7g	5.2±0.1 (2)		2.3±0.1 (2)	2.9
7h	<4.4 (2)		1.2±0.2 (2)	<3.2
7i	5.6±0.04 (2)	4.6±0.1 (2)	4.0±0.4 (3)	1.6
7j	5.8±0.01 (2)		2.9±0 (2)	2.9
7k	6.6±0.2 (3)	6.3±0.1 (2)	2.6±0.1 (2)	4.0
II				
8	5.1±0.03 (2)	<4.5 (2)	>4.2 (2)	<0.9
9a	6.6±0.01 (2)	6.2±0.04 (2)	3.1±0.2 (5)	3.5
9b	<4.4 (1)		1.9±0.2 (3)	<2.5
10	4.9±.0.03 (3)	<4.5 (2)	4.6±0.9 (2)	0.3
15	6.0±0.3 (3)	5.4±0.1 (2)	2.8±0.1 (2)	3.2
III				
18a	6.1±0.03 (2)	5.6±0.1 (3)	3.8±0.2 (4)	2.3
18b	5.8±0.1 (2)	5.0±0.03 (2)	>3.8 (4)	<2.0
18c	6.3±0.1 (2)	5.9±0.1 (2)	>3.9 (2)	<2.4
18d	6.0±0.01 (2)	5.4±0.2 (2)	3.9±0.6 (2)	2.1
18e	5.7±0.1 (2)		>4.8 (2)	<0.9
IV				
11a	<4.4 (2)		0.8±0.1 (2)	<3.6
11b	4.5±0.01 (2)		0.7±0.2 (2)	3.8
27	5.6±0.1 (2)	5.0±0.2 (2)	2.7±0 (2)	2.9
29	6.5±0.1 (2)	6.7±0.1 (2)	3.8±0.1 (3)	2.7
31	5.8±0.2 (2)	5.1±0.1 (2)	2.6±0.1 (2)	3.2
34	5.6±0.1 (2)	5.1±0.1 (2)	1.1±0.1 (2)	4.5

[a] pIC_{50} is reported as mean ± SD, n = 2–4 from ten point CR with the number of experiments in parentheses. [b] LLE was calculated as LLE = $pIC_{50} - logD_{7.4}$.[20]

To further investigate the amidine functionality (II) the reversed amidine (**15**, Scheme 2) was synthesized. Synthesis started from commercially available 4-chloro-2-(chloro-methyl)-1-methoxy-benzene (**12**), which was reacted with cyclopentanethiol, followed by formation of the corresponding benzonitrile and finally amidation to give the desired reversed amidine **15**. Compound **15** drops 1 order of magnitude in activity (Table 2) and indicates that the topology around the positive charge is sensitive.

The SAR exploration was continued at the methoxy position (III, Scheme 3, **18a–18e**). Reacting **16** with cyclopentanethiol followed by reduction of the nitro group gave aniline intermediate **17a**. The methyl substituted aniline (**17b**) was synthesized from **19** by reduction of the carboxylic acid followed by halogenation, reaction with cyclopentanethiol, and reduction of the nitro group. The halo substituted intermediates **17c** and **17d** were synthesized from 2-fluoro or 2-chloro-5-nitrobenzaldehyde (**21a** and **21b**), respectively, by reduction of the aldehyde and subsequent reduction of the nitro group followed by Boc protection of the resulting aniline. Compounds **22a** and **22b** were converted to the corresponding bromides, which were then reacted with cyclopentanethiol, and after Boc deprotection the aniline intermediates **17c** and **17d** were obtained. Nitration of 2- trifluoromethoxybenzaldehyde (**23**) followed by reduction of the aldehyde gave the alcohol **24**. Treatment of the alcohol with methanesulfonyl chloride, subsequent reaction with cyclopentanethiol, and finally reduction of the nitro group gave aniline **17e**. Aniline intermediates (**17a–17e**) were reacted with methyl thiophene-2-carboximidothioate to give the desired amidine analogues (**18a–18e**, Scheme 3). Read-out from the IP-1 assay clearly suggest a steep SAR as all of the methoxy-replacements lost at least 1 order of magnitude as compared to **1** (Table 2).

The final SAR assessment was performed at the cyclopentylsulfanylmethyl group (IV). Sulfur was replaced by classical bioisosters[21] as −O− or $-CH_2-$ giving compounds **27** and **29**, respectively (Scheme 4). Synthesis of compound **27** started with bromomethylation of **4** to give **25**, which after nucleophilic substitution with cyclopentanol furnished the ether (**26**). Reduction of the nitro group and reaction with methyl thiophene-2-carboximidothioate yielded compound **27**. The carbon analogue (**29**) was synthesized from **25** by a Wittig reaction, followed by simultaneous reduction of the nitro group and the double bond using H_2(g) and subsequent reaction with methyl benzenecarboximidothioate. The nonclassical sulfur bioisosteres[21] −SO− and $-SO_2-$ (**11a** and **11b**, respectively, Scheme 1) were accomplished by oxidation of **7b** using 3-chlororbenzoperoxoic acid. Out of the synthesized bioisosteres (**27**, **29**, **11a**, and **11b**), only the carbon analogue (**29**, pIC_{50} 6.5) retained some potency but still lost 1.2 log units compared to **7b** (Table 2).

To challenge polarity, sulfur was replaced by an amide bond exemplified by compound **34** (Scheme 5). The starting material (**32**) was coupled with cyclopentane-carboxylic acid to give the nitrobenzene intermediate (**33**), which after standard reduction of the nitro group and reaction with benzonitrile yielded compound **34**. The increase in polarity ($logD_{7.4}$ = 1.1, $\Delta logD_{7.4}$ = 1.4) was accompanied with an even more pronounced decrease in potency (ΔpIC_{50} = 2.1) compared to the sulfur analogue **7b** (Table 2).

IP-1 data from exploration of the aliphatic cyclopentyl ring suggest a tight SAR also in this region. Nine aryl analogues (data not shown) were made, which all display a potency of 1 μM or less, here exemplified with the phenyl analogue (**31**,

dx.doi.org/10.1021/ml400519h | ACS Med. Chem. Lett. 2014, 5, 527–532

Scheme 1[a]

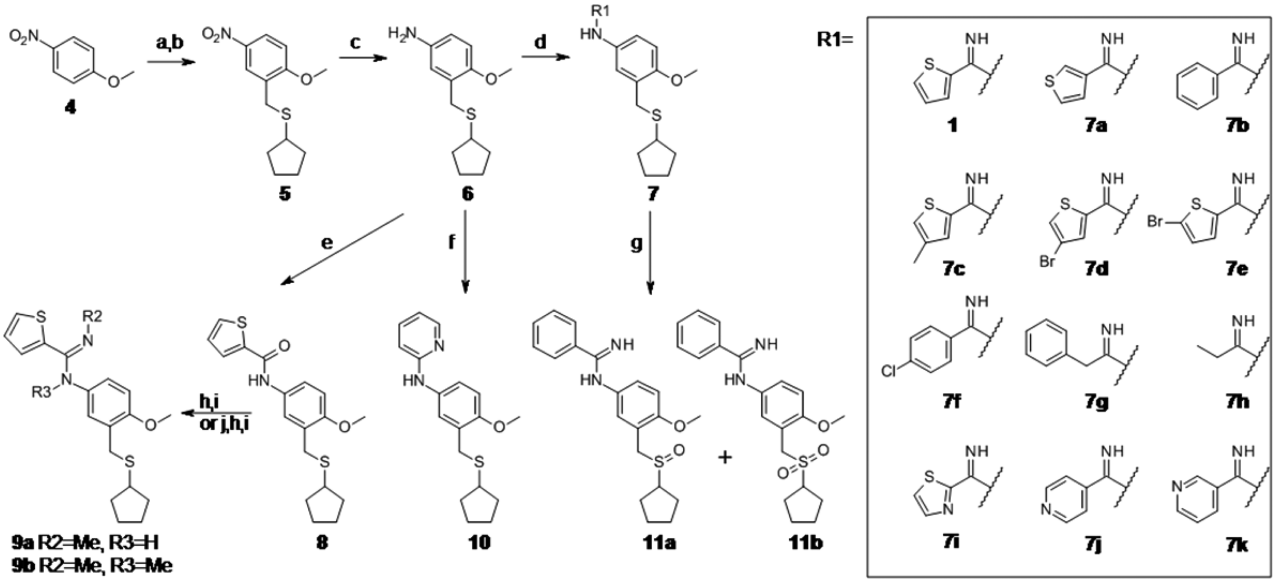

[a]Reagents and conditions: (a) CHO, H_2SO_4, NaBr, HOAc, 85 °C; (b) cyclopentanethiol, K_2CO_3, DMF; (c) iron dust, HOAc, 60 °C; (d) R1−CN, $AlMe_3$, toluene, 95 °C or ethylmagnesium bromide, THF or $AlCl_3$, 1,2-dichlororethane, 115 °C; (e) thiophene-2-carboxylic acid, EDC, HOBt, TEA, DMF; (f) 2-fluoropyridine, Cs_2CO_3, DMA, 200 °C; (g) R1 = benzenecarboximidoyl, 3-chlorobenzoperoxoic acid, DCM; (h) Lawesson reagent, toluene, 80 °C; (i) $MeNH_2$, MeOH, 50 °C; (j) NaH, MeI, THF, 0 °C.

Scheme 2[a]

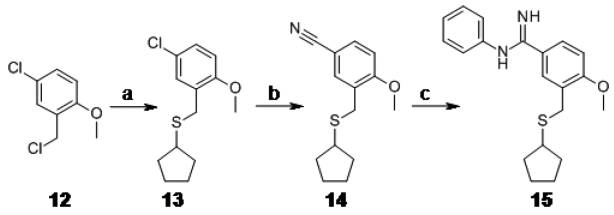

[a]Reagents and conditions: (a) cyclopentanethiol, K_2CO_3, DMF; (b) Zn, $Zn(CN)_2$, XPhos, $Pd_2(dba)_3$, DMA, 150 °C; (c) aniline, $AlMe_3$, toluene, 95 °C.

Scheme 3[a]

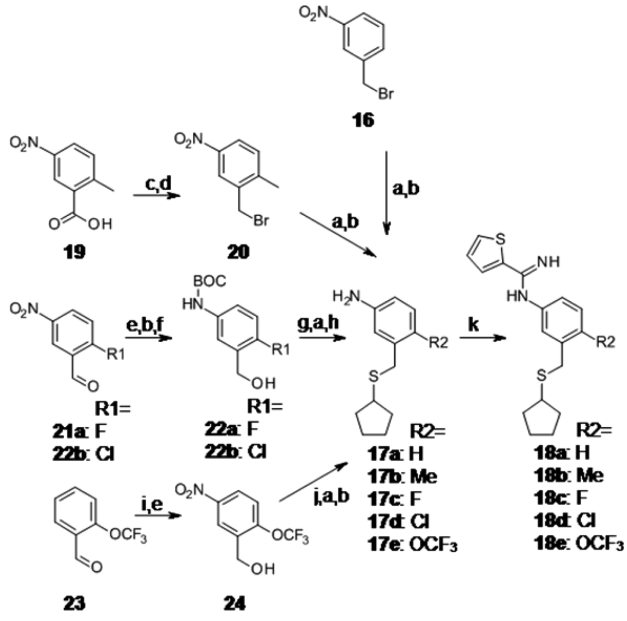

[a]Reagents and conditions: (a) cyclopentanethiol, K_2CO_3 or Cs_2CO_3 or NaOH, DMF or MeOH; (b) iron dust, HOAc or NH_4Cl, 60 °C; (c) BH_3, THF, 30 °C; (d) PBr_3, DCM, 0 °C; (e) $NaBH_4$, THF, MeOH, 0 °C; (f) Boc_2O, DMF, 60 °C; (g) PPh_3, NBS; (h) HCl; (i) H_2SO_4, HNO_3, 0 °C; (j) TEA, DCM, methanesulfonyl chloride; (k) methyl thiophene-2-carboximidothioate, *i*-propanol, 85 °C or thiophene-2-carbonitrile, $AlMe_3$, toluene, 95°.

Scheme 4 and Table 2). Compound **31** was synthesized from **25** by reaction with benzenethiol, followed by reduction of the nitro group using iron dust and reaction of the aniline intermediate with benzonitrile.

Encouraging for this series originating from compound **1**, SAR revealed no consistent correlation between potency and lipophilicity (Table 2). A higher lipophilic ligand efficiency (LLE) indicates less lipophilic contribution to potency and is therefore a suitable way to rank lead compounds.[20] For the best compound (**7b**), LLE could be increased to 5.2. For 20 of the compounds presented in Table 2, GPR103 activity was confirmed in RLB. A good correlation between functional and binding data for these ligands was observed (see Supporting Information, Figure S3).

In summary, an HTS was run with 900,000 compounds targeting GPR103 using an IP-1 assay. After functional screening in IP-1 single concentration and ten point CR followed by orthogonal screening in DMR, the most active and interesting clusters were followed up in a [^{125}I]-QRFP43 RLB ten point CR assay. A low confirmation rate with respect to functional versus affinity data from screening of the initial hit clusters was observed. This led to a revision of the screening cascade to enable affinity screening of a larger set of compounds and secure project progression. The [^{125}I]-QRFP43 RLB assay ten point CR assay was optimized to run in single concentration to enable a larger number of chemical clusters and singletons to be evaluated. This lead to the discovery of several chemically diverse compounds acting as GPR103 antagonists. Herein three new chemical entities

dx.doi.org/10.1021/ml400519h | ACS Med. Chem. Lett. 2014, 5, 527−532

Scheme 4[a]

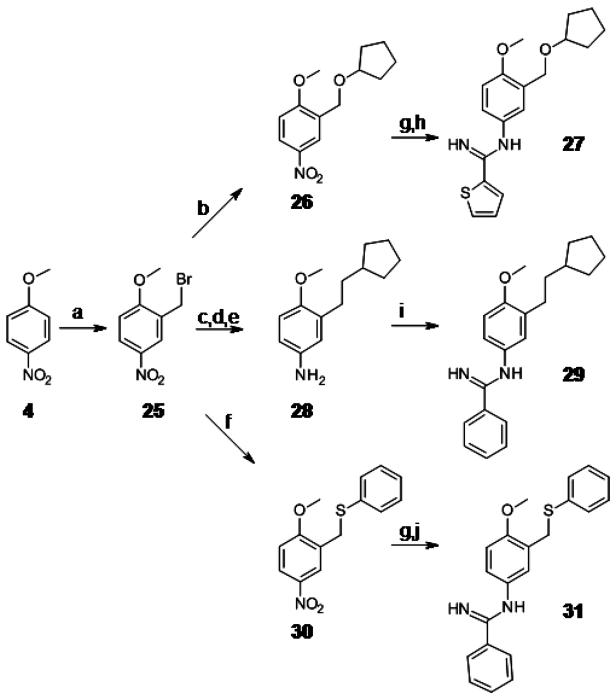

[a]Reagents and conditions: (a) CHO, H_2SO_4, NaBr, HOAc, 85 °C; (b) cyclopentanol, *t*-BuOK, THF, 50 °C; (c) PPh_3, DMF, 100 °C; (d) cyclopentanecarbaldehyde, *t*-BuOK, THF, 0 °C; (e) Pd/C, H_2(g), MeOH, 25 °C; (f) benzenethiol, K_2CO_3, DMF; (g) iron dust, HOAc, 70 °C; (h) methyl thiophene-2-carboximidothioate, *i*-propanol, Δ; (i) methyl benzenecarboximidothioate, *i*-propanol, 88 °C; (j) benzonitrile, $AlMe_3$, toluene, 95 °C.

Scheme 5[a]

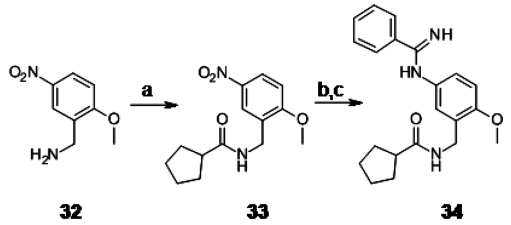

[a]Reagents and conditions: (a) cyclopentanecarboxylic acid, TBTU, DIEA, DMF/DCM, 0 °C–rt; (b) iron dust, HOAc, 60 °C; (c) benzonitrile, $AlMe_3$, toluene, 95 °C.

structurally distinct from disclosed GPR103 antagonists[13−16] are reported. For one of the hits, *N*-[3-(cyclopentylsulfanyl-methyl)-4-methoxy-phenyl]thiophene-2-carboximidamide (**1**), we present SAR exploration resulting in the finding of structural features important for the activity of this compound class.

■ ASSOCIATED CONTENT

Supporting Information

Figures S1, S2 and S3, an enlarged version of Table 2 with structures drawn in the table, detailed information on synthetic procedures, and characterization of compounds as well as description of biological assays associated with this communication. This material is available free of charge via the Internet at http://pubs.acs.org.

■ AUTHOR INFORMATION

Corresponding Author

*(K.A.N.) Tel: +46 31 7762426. Fax: +46 31 7763700. E-mail: kristina.a.nilsson@astrazeneca.com.

Notes

The authors declare no competing financial interest.

■ ACKNOWLEDGMENTS

The authors would like to thank Bryan Egner for synthesis of 2-hydroxy-5-nitro-benzaldehyde. We would also like to thank the Separation Science Group at AstraZeneca Mölndal for help with compound purification.

■ ABBREVIATIONS

CR, concentration response; DIEA, ethyldiisopropylamine; DMR, dynamic mass redistribution; EDC, 3-(ethylimino-methylene-amino)-*N*,*N*-dimethyl-propan-1-amine; GPR103, pyroglutamylated RF amide peptide receptor 103; HOAc, acetic acid; HOBt, 1-hydroxybenzotriazole; IP-1, inositol-1-phosphate; LLE, lipophilic ligand efficiency; $logD_{7.4}$, logarithm of the distribution coefficient measured at pH 7.4; RLB, radio ligand binding; TBTU, 2-(1*H*-benzo[*d*][1,2,3]triazol-1-yl)-1,1,3,3-tetramethyl-isouronium tetrafluoroborate; TEA, triethyl-amine

■ REFERENCES

(1) Finucane, M. M.; Stevens, G. A.; Cowan, M. J.; Danaei, G.; Lin, J. K.; Paciorek, C. J.; Singh, G. M.; Gutierrez, H. R.; Lu, Y.; Bahalim, A. N.; Farzadfar, F.; Riley, L. M.; Ezzati, M. National, regional, and global trends in body-mass index since 1980: systematic analysis of health examination surveys and epidemiological studies with 960 country-years and 9.1 million participants. *Lancet* **2011**, *377*, 557−67.

(2) Nguyen, D. M.; El-Serag, H. B. The epidemiology of obesity. *Gastroenterol. Clin. North Am.* **2010**, *39*, 1−7.

(3) Lee, D. K.; Nguyen, T.; Lynch, K. R.; Cheng, R.; Vanti, W. B.; Arkhitko, O.; Lewis, T.; Evans, J. F.; George, S. R.; O'Dowd, B. F. Discovery and mapping of ten novel G protein-coupled receptor genes. *Gene* **2001**, *275*, 83−91.

(4) Jiang, Y.; Luo, L.; Gustafson, E. L.; Yadav, D.; Laverty, M.; Murgolo, N.; Vassileva, G.; Zeng, M.; Laz, T. M.; Behan, J.; Qiu, P.; Wang, L.; Wang, S.; Bayne, M.; Greene, J.; Monsma, F., Jr; Zhang, F. L. Identification and characterization of a novel RF-amide peptide ligand for orphan G-protein-coupled receptor SP9155. *J. Biol. Chem.* **2003**, *278*, 27652−27657.

(5) Fukusumi, S.; Yoshida, H.; Fujii, R.; Maruyama, M.; Komatsu, H.; Habata, Y.; Shintani, Y.; Hinuma, S.; Fujino, M. A new peptidic ligand and its receptor regulating adrenal function in rats. *J. Biol. Chem.* **2003**, *278*, 46387−46395.

(6) Chartrel, N.; Dujardin, C.; Anouar, Y.; Leprince, J.; Decker, A.; Clerens, S.; Do-rego, J.; Vandesande, F.; Llorens-Cortes, C.; Costentin, J.; Beauvillain, J.; Vaudry, H. Identification of 26RFa, a hypothalamic neuropeptide of the RFamide peptide family with orexigenic activity. *Proc. Natl. Acad. Sci. U.S.A.* **2003**, *100*, 15247−15252.

(7) Le Olivier, M.; Neveu, C.; Lefranc, B.; Dubessy, C.; Boutin, J. A.; Do-Rego, J.; Costentin, J.; Tonon, M.; Tena-Sempere, M.; Vaudry, H.; Leprince, J. Structure−activity relationships of a series of analogues of the RFamide-related peptide 26RFa. *J. Med. Chem.* **2011**, *54*, 4806−4814.

(8) Bruzzone, F.; Lectez, B.; Alexandre, D.; Jegou, S.; Mounien, L.; Tollemer, H.; Chatenet, D.; Leprince, J.; Vallarino, M.; Vaudry, H.; Chartrel, N. Distribution of 26RFa binding sites and GPR103 mRNA in the central nervous system of the rat. *J. Comp. Neurol.* **2007**, *503*, 573−591.

(9) Chartrel, N.; Alonzeau, J.; Alexandre, D.; Jeandel, L.; Alvear-Perez, R.; Leprince, J.; Boutin, J.; Vaudry, H.; Anouar, Y.; Llorens-

Cortes, C. The RFamide neuropeptide 26RFa and its role in the control of neuroendocrine functions. *Front. Neuroendocrinol.* **2011**, *32*, 387−397.
(10) Takayasu, S.; Sakurai, T.; Iwasaki, S.; Teranishi, H.; Yamanaka, A.; Williams, S. C.; Iguchi, H.; Kawasawa, Y. I.; Ikeda, Y.; Sakakibara, I.; Ohno, K.; Ioka, R. X.; Murakami, S.; Dohmae, N.; Xie, J.; Suda, T.; Motoike, T.; Ohuchi, T.; Yanagisawa, M.; Sakai, J. A neuropeptide ligand of the G protein-coupled receptor GPR103 regulates feeding, behavioral arousal, and blood pressure in mice. *Proc. Natl. Acad. Sci. U.S.A.* **2006**, *103*, 7438−7443.
(11) Jean-Claude, R.; Leprince, J.; Chartrel, N.; Vaudry, H.; Costentin, J. Behavioral effects of 26RFamide and related peptides. *Peptides* **2006**, *27*, 2715−2721.
(12) Neveu, C.; Lefranc, B.; Tasseau, O.; Do-Rego, J.; Bourmaud, A.; Chan, P.; Bauchat, P.; Marec, O. L.; Chuquet, J.; Guilhaudis, L.; Boutin, J. A.; Segalas-Milazzo, I.; Costentin, J.; Vaudry, H.; Baudy-Floc'h, M.; Vaudry, D.; Leprince, J. Rational design of a low molecular weight, stable, potent, and long-lasting GPR103 aza-beta3-pseudopeptide agonist. *J. Med. Chem.* **2012**, *55*, 7516−7524.
(13) Haga, Y.; Mizutani, S.; Sato, N. Preparation of indole-2-carboxamide derivatives as QRFP receptor (GPR103) antagonists. WO2010126164A1, 11/040, 2010.
(14) Fujimura, T.; Kishino, H.; Mizutani, T.; Sakuraba, S.; Sasaki, T.; Sato, N. Preparation of (hetero)aryl-substituted indolecarboxamides as GPR103 antagonists. WO2010119984A1, 10/21, 2010.
(15) Kishino, H.; Mizutani, S.; Sakuraba, S.; Sato, N. Preparation of aryl indole derivatives as human QRFP receptor (GPR103) antagonists. WO2010117085A1, 10/14, 2010.
(16) Haga, Y.; Moriya, M.; Takahashi, T. Preparation of arylimidazoline for use as antiobesity agents. WO2010123150A1, 10/28, 2010.
(17) Nordvall, G.; Petersson, C.; Rakos, L.; Sohn, D. Novel 8-sulfonyl-3-amino-substituted chroman or tetrahydronaphthalene derivatives modulating the 5-HT6 receptor and their preparation and pharmaceutical compositions. WO2006126938A1, 11/30, 2006.
(18) Webb, T. R.; Lvovskiy, D.; Kim, S.; Ji, X.; Melman, N.; Linden, J.; Jacobson, K. A. Quinazolines as adenosine receptor antagonists: SAR and selectivity for A2B receptors. *Bioorg. Med. Chem.* **2003**, *11*, 77−85.
(19) Pierry, C.; Couve-Bonnaire, S.; Guilhaudis, L.; Neveu, C.; Marotte, A.; Lefranc, B.; Cahard, D.; Segalas-Milazzo, I.; Leprince, J.; Pannecoucke, X. Fluorinated pseudopeptide analogues of the neuropeptide 26RFa: synthesis, biological, and structural studies. *ChemBioChem* **2013**, *14*, 1620−1633.
(20) Leeson, P. D.; Springthorpe, B. The influence of drug-like concepts on decision-making in medicinal chemistry. *Nat. Rev. Drug Discovery* **2007**, *6*, 881−890.
(21) Meanwell, N. A. Synopsis of some recent tactical application of bioisosteres in drug design. *J. Med. Chem.* **2011**, *54*, 2529−2591.